Macromolecules

ARTICLE

pubs.acs.org/Macromolecules

Role of Interfacial Interaction in Orientation of Poly(*N*-isopropylacrylamide) Chains on Silicon Substrate.

C.-H. Wang,[†] S. Mukherjee,[§,∥] A. K. M. Maidul Islam,[§] Y.-W. Yang,[†,‡] and M. Mukherjee*[,§]

[†]National Synchrotron Radiation Research Center, Hsinchu 30077, Taiwan

[‡]Department of Chemistry, National Tsing-Hua University, Hsinchu 30013, Taiwan

[§]Surface Physics Division, Saha Institute of Nuclear Physics, 1/AF Bidhannagar, Kolkata 700064, India

ABSTRACT: Studies of self-assembled PNIPAM films on hydrophilic and hydrophobic substrates that are grown below and above lower critical solution temperature (LCST) have been performed to understand the role of intramolecular and polymer−substrate interactions in self-assembly using near edge X-ray absorption fine structure (NEXAFS) spectroscopy, atomic-force microscopic (AFM) and density functional theory (DFT). The NEXAFS spectra suggest that the polymer chains are oriented similarly on hydrophilic as well as hydrophobic substrate although the chains were having different morphologies in the solution, whereas, AFM studies shows that the morphology of the polymer chains on the two substrates are widely different. NEXAFS absorption spectra for free molecule and that with effects of substrate were calculated using DFT. The results show that on hydrophobic substrate polymer−substrate interaction is stronger as compared to that with hydrophilic one, however, for both cases this interaction plays dominant role over the intramolecular interaction for the orientation of the chains on the substrate. Matching of the calculated and experimental NEXAFS spectra shows on both types of substrates only a fraction of the attached molecules are oriented. Effect of external force on polymer substrate attachment was studied with the spin-coated films on hydrophilic substrate. Our results show that in this case substrate attachment plays an important role unlike the case of self-assembly on hydrophilic substrate, where the polymer−substrate interaction is weak.

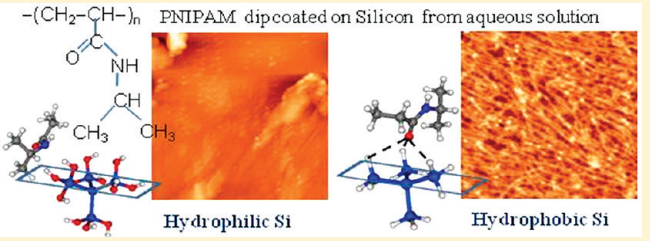

INTRODUCTION

Stimuli-responsive polymers are materials that show potential for well-designed surfaces and interfaces for a wide range of applications from medicine[1] to nanotechnology.[2,3] Response to different physical factors in these materials are known, for instance, response to pH,[4] magnetic field[5] or to temperature[6] changes. Poly(*N*-isopropylacrylamide) (PNIPAM) is a widely studied thermo sensitive polymer.[7−20] This polymer in water exhibits a reversible[21] phase transition at a lower critical solution temperature (LCST). The solution behavior of PNIPAM has been investigated by a variety of experimental techniques in the dilute and concentrated regimes. The LCST of PNIPAM in water is approximately at 32 °C which is close to human body temperature, which makes PNIPAM an attractive temperature-sensitive polymer for the study of biomedical applications.[22] Recently poly(*N*-isopropylacrylamide)-grafted hyaluronan (PNIPAM−HA) and PNIPAM-grafted gelatin (PNIPAM−gelatin), which exhibit sol-to-gel transformation at physiological temperature, were applied as tissue adhesion prevention material and hemostatic aid, respectively.[23]

The temperature-dependent change in the conformation of PNIPAM chains reflects changes in polymer/water interactions. At lower temperatures, intermolecular hydrogen bonds between solvent water and polar groups of PNIPAM keep the polymer soluble. At higher temperature above the LCST the hydrogen bonds break, and hydrophobic associations between the collapsed polymer chains take place. Several models have been described to account for the coil-to-globule transition of PNIPAM in water and the complex water/PNIPAM phase diagram.[24−26] It has recently been stressed that PNIPAM is never completely hydrophobic.[27] In fact, as mentioned by the author, PNIPAM is not completely hydrophilic—it has hydrophilic and hydrophobic domains above and below the LCST. Like amphiphilic proteins and surfactants, oxygen and nitrogen rich domains of PNIPAM are hydrophilic above and below the LCST. Similarly the isopropyl groups and the polymethylene backbones are hydrophobic above and below the LCST.

It is therefore clear that even if the polymer is not completely hydrophilic or hydrophobic, it shows an overall hydrophilic/hydrophobic nature across LCST in water due to the nature of intramolecular interaction. However, from both fundamental as well as application point of view it is important to understand whether intramolecular force or the molecule substrate interaction would play a dominant role if the polymer at a particular morphology (hydrophilic or hydrophobic) is allowed to interact with a hydrophobic/hydrophilic substrate. Motivated by the above question here we have studied self-assembled PNIPAM films on hydrophilic and hydrophobic substrates. Our observation

Received: March 17, 2011
Revised: June 4, 2011
Published: June 24, 2011

shows the substrate−polymer interaction plays a dominant role as compared to the intramolecular interaction when the polymer molecules self-assemble on Si substrate.

SAMPLE PREPARATION

Organic films of PNIPAM (Aldrich, molecular weight, M_n 20 000−25 000) were prepared by adsorbing on hydrophilic and hydrophobic silicon substrates at temperatures below and above the lower critical solution temperature (LCST). Silicon substrates were made hydrophilic according to RCA cleaning procedure by boiling the substrate in a solution of ammonium hydroxide (Merck, 98%), hydrogen peroxide (Merck, 98%), and Milli-Q water ($H_2O/NH_4OH/H_2O_2$ = 2/1/1 by volume) for 10 ± 1 min. Hydrophobic substrates were prepared by etching the native oxide by dilute (10%) hydrofluoric acid (HF) for 3 min. This procedure makes the silicon H-terminated and produces the hydrophobic surfaces. Freshly cleaned substrates were immersed into beakers containing different aqueous PNIPAM solutions of concentration 1 mg/mL for about 2 h. The coated substrates were then dipped in clean water for 1 h to remove any loosely bound entity followed by drying in air. Two samples were prepared by adsorption at temperature 8 °C (below LCST) in a refrigerator on hydrophilic (sample 1) and hydrophobic (sample 2) silicon substrate. Above LCST, another two samples were prepared at 60 °C in an oven on hydrophilic (sample 3) and hydrophobic (sample 4) silicon substrates. For both cases the PNIPAM solutions were prepared and maintained at the desired temperatures before the freshly prepared substrates were dipped in them. Thickness of all the films were measured by using AFM scans across cut marks on the samples. The thickness of the films on HF treated substrates are 5.4 ± 1 nm (8 °C) and 12.6 ± 1 nm (60 °C), whereas the films on the RCA treated samples ware very thin and the thickness was not measurable by this technique. Two spin-coated PNIPAM samples on hydrophilic substrates with thickness around 30 nm were also prepared from solutions of concentration 5 and 15 mg/mL referred to as sample 5 and 6 respectively.

EXPERIMENTAL SECTION

All the sample characterization was performed at the National Synchrotron Radiation Research Center (NSRRC), Taiwan. Atomic force microscope (AFM) imaging was carried out at room temperature and ambient condition with a Veeco Innova Scanning Probe Microscope operated in tapping mode. X-ray photoemission spectroscopy (XPS) spectra were acquired with a SPEC PHOBIOS 150 electron energy analyzer mounted in a mu-metal surface science chamber in Wide-Range beamline (BL24A) of NSRRC. Near-edge X-ray absorption fine structure (NEXAFS) spectroscopy was performed at room temperature with a home-built partial electron yield (PEY) detector constructed with a microchannel plate in conjunction with three meshes for voltage-biasing purpose. The retarding voltages are chosen to allow Auger electrons of interest to be registered in the microchannel plate. For the three absorption edges of PNIPAM investigated here, the retarding potentials are set at −150, −300, and −400 V for carbon, nitrogen, and oxygen edges, respectively. The polarization dependence of NEXAFS were obtained by varying the X-ray incident direction between normal incidence (θ = 90°) and glancing incidence (θ = 20°). Different data were collected from different positions on the sample surface to minimize the effect of beam damage. Time-varying incident photon flux (I_{mesh}) was monitored with a gold mesh. Spectra were first normalized to flux variation by dividing the sample current with the corresponding mesh current, the so-called I_{mesh} normalization. However, for carbon NEXAFS data, due to the presence of carbons in the beamline optical components and gold mesh, a second normalization was required. The $I_{sample}(\hbar\omega)$ was normalized to the drain current from a clean gold sample ($I_{Au}(\hbar\omega)$, featuring an unstructured absorption cross section[28,29] in the energy range of interest) as follows, $A(\hbar\omega) = (I_{sample}(\hbar\omega,t)/I_{mesh}(\hbar\omega,t)) \times (I_{mesh}(\hbar\omega,t')/I_{mesh}(\hbar\omega,t'))$, where t and t' represent the two different times when the sample and the clean gold were measured, respectively. It needs to be stressed that, during various stages of spectrum normalization, a careful alignment of photon energy scale among different runs must be ensured, or else the spurious features would emerge.

COMPUTATIONAL METHODS

The equilibrium geometry and X-ray absorption spectra (C and N 1s) of the molecule were calculated by DFT with the computer code STOBE[30] The effect of the substrate was included through a cluster consisting of 1 central Si atom surrounded by 4 SiH units. A gradient corrected RPBE exchange/correlation functional was applied.[31,32] To calculate the equilibrium geometry and the X-ray absorption spectra, we used all-electron triple-ζ valence plus polarization (TZVP) atomic Gaussian basis sets for carbon, nitrogen, oxygen and silicon centers, while the hydrogen basis sets were chosen to be of the double-ζ (DZVP) type.[33] The starting geometries for the optimization procedure was obtained using ACD/ChemSketch (http://acdlabs.com/products/draw_nom/draw/chemsketch/) and Vega ZZ (http://www.ddl.unimi.it/). To calculate X-ray absorption spectra, the Slater transition state method was applied.[34,35] In this case the optimized geometry obtained from the geometry optimization calculation was kept fixed and polarization and angle dependent absorption spectra were calculated. In order to obtain an improved representation of relaxation effects in the inner orbitals, the ionized center was described by using the IGLO-III basis.[36] A diffuse even-tempered augmentation basis set was finally included at the excitation center to account for transitions to unbound resonances. The NEXAFS spectra were generated through a Gaussian convolution of the discrete spectra with varying broadenings. For an energy range 9−10 eV near the ionization threshold the broadening (FWHM) was set to 1.0 eV and for the remaining part of the spectrum the FWHM was linearly increased up to 20 eV with energy.

RESULTS AND DISCUSSION

In Figure 1, the AFM images of the samples prepared by adsorption on hydrophilic and hydrophobic substrates at low and high temperatures are shown. It can be observed from the images that on hydrophilic substrate the coverage is low (film thickness cannot be measured, as mentioned before) and the polymer molecules form isolated clusters whereas on the hydrophobic substrate chain-like elongated structures are formed. While maintaining the morphology, the coverage was found to increase at higher temperature for both substrates. This behavior of self-assembly indicates that the nature of the substrate plays the major role in determining the morphology of the polymer molecules on the surface.

Below the LCST, the polymer is hydrophilic, and by the general notion, we believe it is likely that it would be more attracted on a hydrophilic substrate at this stage; however, what we observe is different, even at this stage the polymer prefers hydrophobic substrate over hydrophilic one. It appears that although the chain morphology in the solution at lower temperature is different compared to that of higher, this does not influence the nature of the self-assembled structure. Very low coverage on hydrophilic substrate in both temperatures suggests that when interacting with a substrate, PNIPAM prefers a hydrophobic surface over a hydrophilic one ignoring its own internal morphology or philicity in water.

In Figure 2, we have shown the XPS survey scan spectrum for a PNIPAM sample (sample 3). The spectrum shows that the

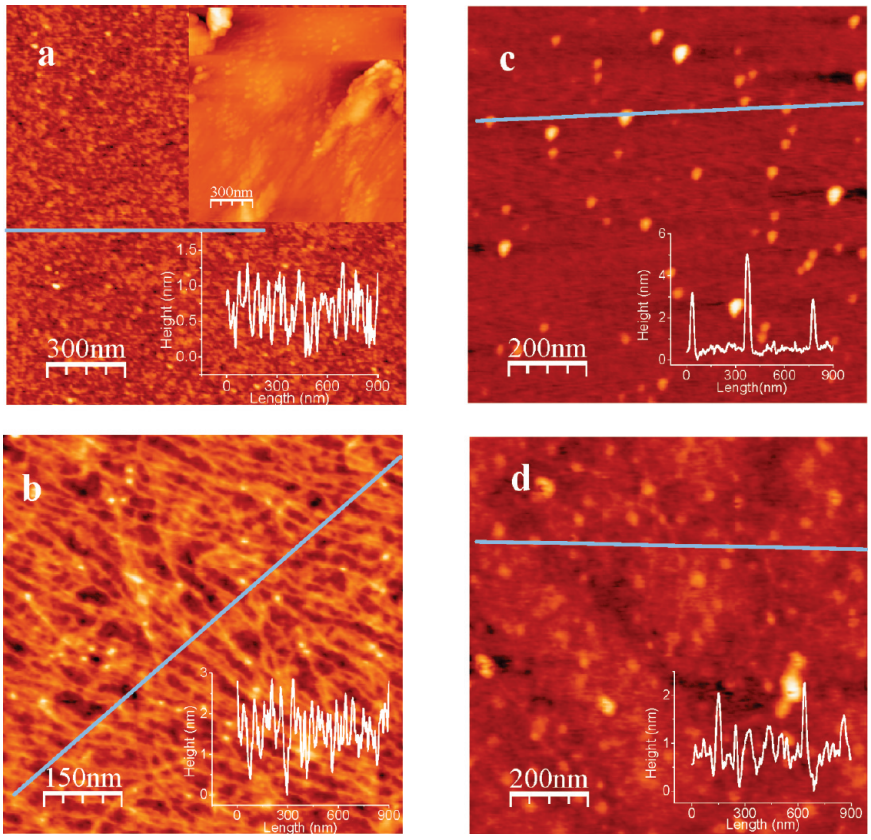

Figure 1. AFM images of samples prepared by adsorption at 8 °C on (a) hydrophilic substrate and (b) on hydrophobic substrate; samples adsorbed at temperature 60 °C on (c) hydrophilic and (d) on hydrophobic substrates. The line profiles are shown at the inset of the corresponding figure.

sample is clean and atomic concentrations agree well with the chemical compositions of the material. Oxygen data are not shown as it is present on the substrate surface also.

It is noteworthy that the NEXAFS spectra for samples prepared at high and low temperature do not show any qualitative difference. Therefore, in Figure 3 we have shown the C and N K-edge NEXAFS spectra for samples 3 and 4, prepared at higher temperature and sample 6 (spin-coated) for the two different orientations of the electric field vector with respect to the surface. The difference in spectra for different orientations of the field vector is a clear indication that the polymer molecules are oriented on the surface in a specific manner. The main features of the C K-edge spectra for all the samples are the following. When the electric field was aligned parallel to the film surface the intensity of the sharp π^* transition at about 288.5 eV for all the samples was found to be higher in comparison to that of the perpendicular orientation of the field. A small peak at low energy around 285 eV in C K-edge spectra was attributed to the radiation damage effect of the samples because its intensity increases with the prolonged X-ray exposure. For N K-edge, the N−H σ bond which has a π-like character due to the orientation of the lone electron pair in the nitrogen atom, exhibits a π-like sharp σ^* transition around 401.5 eV. This transition shows higher intensity compared to broad C−N σ^* transition when the electric field is parallel to the surface for all the samples. However, a careful observation to the C−N σ^* transition peak indicates that there is a clear difference in the nature of this peak between the films that are self-assembled on hydrophilic and hydrophobic substrate (Figure 3, parts a and b). In case of

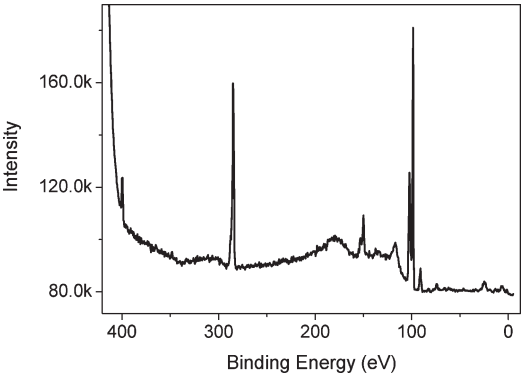

Figure 2. XPS survey scan for adsorbed sample on hydrophilic substrate (sample 3).

hydrophilic substrate there are two major peaks with the one at lower energy being higher in intensity whereas on hydrophobic substrate this region shows three clear peaks with increasing intensity with energy. Furthermore, it is curious to note that the N K-edge spectra for the spin coated sample shown in Figure 3c, which was spun on a hydrophilic silicon substrate, shows similar behavior that was observed for self-assembled films on hydrophobic substrate.

In Figure 4, we have shown the O−K edge spectra of high temperature sample at two different field orientations as a typical case. It may be noted that the variation of the spectra with respect to the electric field orientation is similar in nature to those of

dx.doi.org/10.1021/ma200614w |*Macromolecules* 2011, 44, 5750–5757

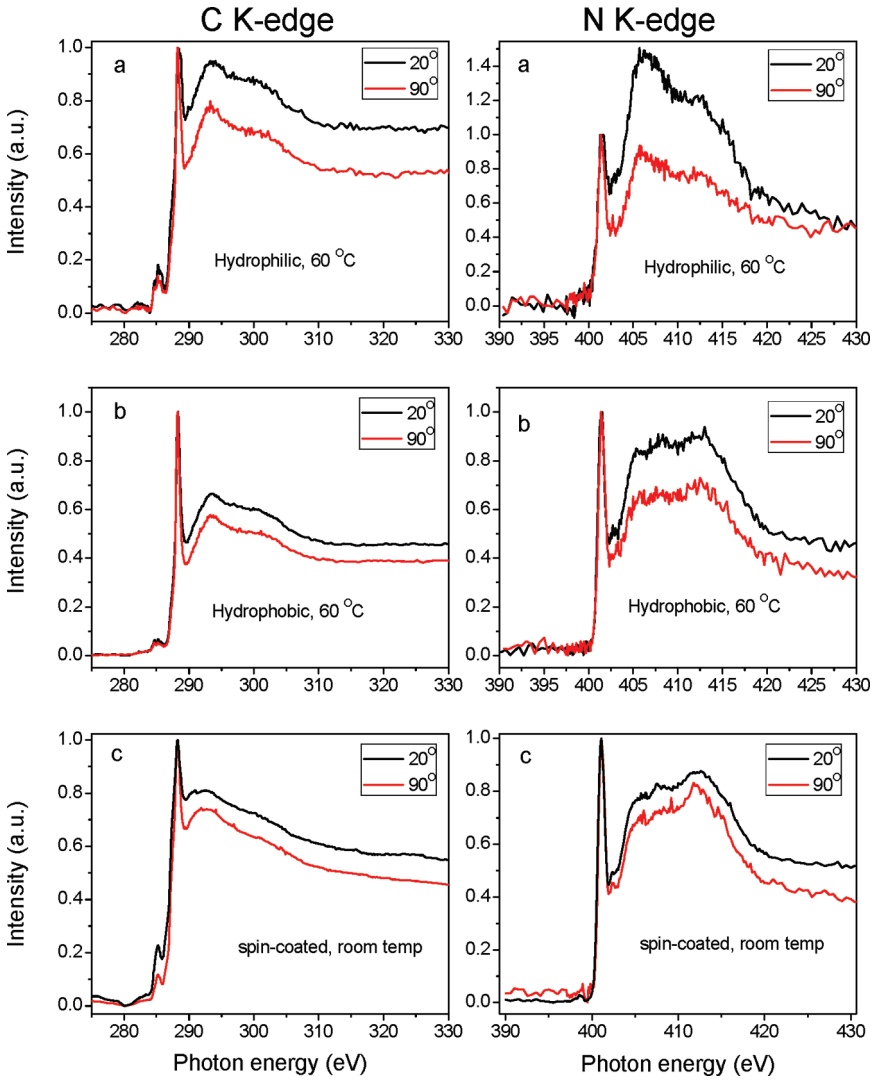

Figure 3. Representative C and N K-edge NEXAFS spectra for samples prepared by (a) adsorption on hydrophilic and (b) hydrophobic substrates and (c) spin-coating on hydrophilic substrate for the two different X-ray incident angles. Normal incidence (θ = 90°) and glancing incidence (θ = 20°) indicates parallel and nearly perpendicular orientations of the electric field vector with respect to the sample surface, respectively. All spectra are normalized to the height of the first sharp peak (instead of same edge-jump) for clarity of discussion.

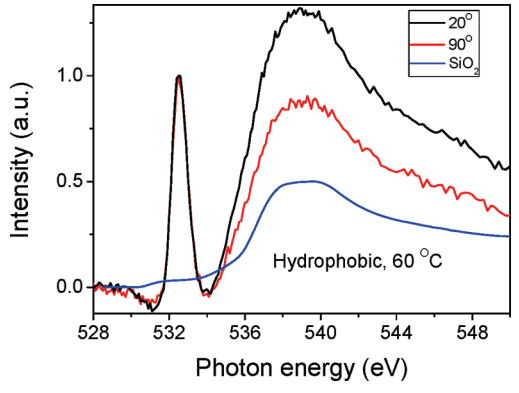

Figure 4. Typical O K-edge NEXAFS spectra for adsorbed sample on hydrophobic substrate. X-ray spectrum of the native oxide present on the substrate surface is shown by the solid blue line.

carbon and nitrogen spectra. However, the absorption band from the oxides on the silicon surface appears close to the σ^* transitions of the polymer as shown in the figure. Therefore, no conclusion was drawn from the O K-edge data.

It may be noted that the morphology of the polymer chains in water are different below and above the LCST. Below LCST, the chains are soluble and extended whereas above LCST they are insoluble and globular in nature. The NEXAFS spectra indicate that although the polymer chains were having different morphologies in the solution, they are oriented in a similar fashion on hydrophilic as well as hydrophobic substrate. This indicates that the substrate−polymer interaction plays a dominant role as compared to the intramolecular interaction when the polymer molecules self-assemble on Si substrate. However the difference in the AFM data for the self-assembly on two substrates indicates that there is some salient difference between the two cases. The NEXAFS results suggest that the planar CONH parts of the polymer chains are oriented in out-of-plane direction perpendicular to the substrate surface. It may be speculated that both H-terminated hydrophobic as well as OH-terminated hydrophilic substrates may take part in hydrogen bonding or dipole type

dx.doi.org/10.1021/ma200614w |*Macromolecules* 2011, 44, 5750–5757

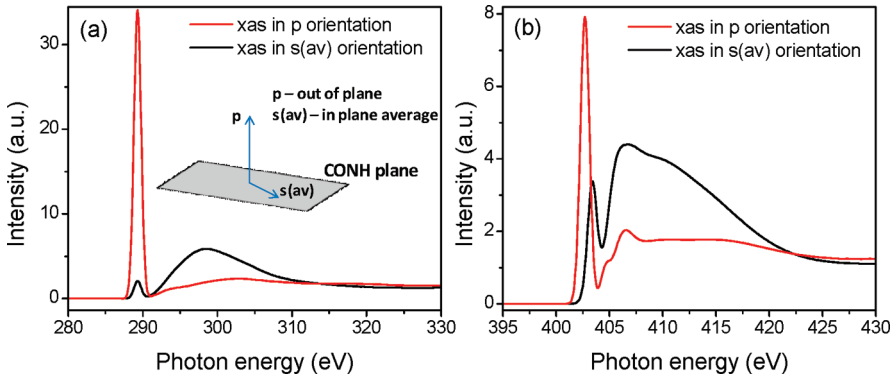

Figure 5. Effect of electric field orientation with respect to CONH plane as obtained from X-ray absorption spectra (XAS) calculations at (a) C K-edge and (b) N K-edge on free PNIPAM molecule containing three monomer units. The inset shows the different orientations of the electric field considered[37] for the calculations.

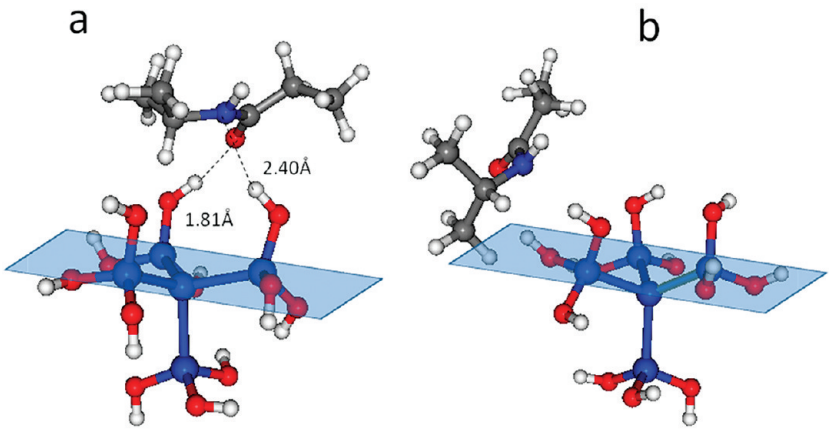

Figure 6. Geometry-optimized molecular models for samples grown on hydrophilic substrate. Atomic distances between the oxygen and nitrogen atoms and the surface hydrogen atoms are indicated. The plane in the figures indicates the position of silicon surface. Color code: hydrogen (white), carbon (gray), oxygen (red), nitrogen (small blue), and silicon (large blue).

interaction with the oxygen or the nitrogen atoms of the CONH groups in the polymer side chains. Therefore, it is likely that the CONH group can have different orientations with respect to the substrate, in other words, either the oxygen or the nitrogen atom may have closer proximity to the substrate. There is another possibility of orientation in which both oxygen and nitrogen atoms are at similar distances from the substrate, in which case the CONH plane should lie parallel to the substrate. However, the experimental observations do not support the latter possibility as a major event.

CALCULATIONS

In order to substantiate the experimental findings and to understand the situation in a better way, we have performed theoretical investigations. It has been observed from the calculation that when the electric field direction is made perpendicular to the CONH plane the C═O π^* and N−H σ^* transitions become pronounced whereas these peaks reduce substantially when the field direction is parallel to the plane as shown in Figure 5. However, for the polymer samples it is unlikely that all the CONH groups will be aligned in a particular direction as there is entanglement of the chains. It is possible that some part of the polymer chain in the films would have random orientation with respect to the field direction. Therefore, the resultant spectrum should be a weighted average of the aligned and randomly oriented molecules.

For calculation of absorption spectra on hydrophilic substrate, a hydrogen-terminated monomer unit was taken. The effect of hydrophilic substrate was introduced through a weakly interacting cluster of five Si atoms where four outer atoms have dangling OH groups. The geometry optimization calculation shows that in one possible configuration hydrogen bonding with bond distances of 1.81 Å between the oxygen atom of the molecule and a hydrogen atom of the OH group of the substrate is likely to occur as shown in Figure 6a. In this configuration the CONH plane is at an oblique direction to the surface. However, another possible configuration as shown in Figure 6b is obtained where the molecule does not show affinity toward the substrate, rather it tend to deviate away from the surface. It was interesting to note that none of these configurations could generate the observed NEXAFS spectra correctly.

The segregated clusters on the hydrophilic substrate observed from AFM suggest that the configuration shown in Figure 6b is more likely in these films. However, although configuration shown in Figure 6a is not preferred in this case, it is responsible

dx.doi.org/10.1021/ma200614w |*Macromolecules* 2011, 44, 5750–5757

for the attachment of the chains to the substrate. Combining the AFM observation and the calculated configurations it may be assumed that only a few segments of the chains interact with the substrate and the rest majority remains free in this case. With this model in mind, calculations were attempted with free polymer molecules and a reasonably good agreement between the theoretical absorption spectra and experimental data was observed when the polymer chain in the calculation was modeled with three monomer units. It was interesting to note that the CONH plane orients nearly parallel to each other for the three units in the optimized geometry. This indicates that if one segment is oriented to the substrate in a manner shown in Figure 6a several following segments will be aligned in a similar way. It can be understood from the calculated configurations that all the molecules are unlikely to be oriented in a particular direction. We observed that a combination of 25% oriented and 75% random molecules was in good agreement with experimental data. In Figure 7, we have shown the comparison between the experimental data for sample 3 grown on hydrophilic substrate with the calculated absorption spectra. It may be noted from the figure that matching between the theoretical and experimental results are much better in case of nitrogen (Figure 7b) as compared to carbon (Figure 7a). This may be explained in terms of the fact that there is only one nitrogen atom per monomer unit of the polymer and all the contribution to the spectrum are due to this atom.

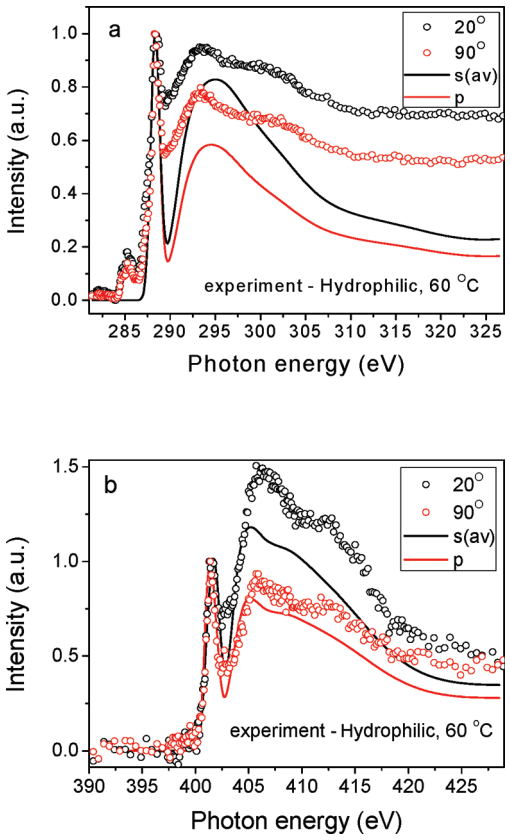

Figure 7. Comparison between the experimental data for sample 3 on hydrophilic substrate with the calculated absorption spectra: (a) C−K edge; (b) N−K edge. A chain of three monomer units terminated with hydrogen atoms was used for the calculation.

Therefore, correct modeling of this single atom in the calculation is expected to reproduce the NEXAFS data correctly. On the other hand there are six carbon atoms in a monomer unit, and the NEXAFS data are a sum of contributions from all of them. As the orientation of a specific atom is important for the absorption calculation, we have taken only three atoms (one in the CONH unit and other two adjacent to it) that are likely to form a planar structure in the calculation. The mismatch between the calculation and the experimental data for carbon (Figure 7a) are possibly due to exclusion of contribution of the other three carbon atoms due to their unknown orientation.

It has been mentioned earlier that the chain-like structures observed in AFM for films deposited on hydrophobic substrate was due to strong substrate polymer interaction. Therefore, for the calculation of the absorption spectra for films on hydrophobic substrate, the effect of hydrogen passivated silicon surface was introduced. The effect of hydrophobic substrate was introduced through a cluster of five Si atoms with four outer atoms having dangling H atoms. The molecular models optimized by the calculation are shown schematically in Figure 8. It can be observed from Figure 8a that the CONH plane is standing vertically on the SiH surface with the oxygen atom pointing downward between the three surface hydrogen atoms. The atomic distances between the oxygen atom and the surface

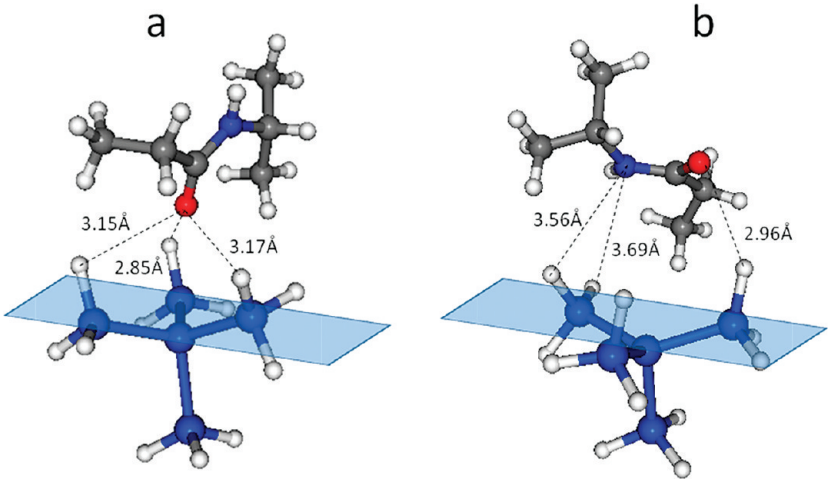

Figure 8. Geometry-optimized molecular models for samples grown on hydrophobic substrate. Atomic distances between the oxygen and nitrogen atoms and the surface hydrogen atoms are indicated. The plane in the figures indicates the position of silicon surface. Color code: same as Figure 6.

dx.doi.org/10.1021/ma200614w |*Macromolecules* 2011, 44, 5750–5757

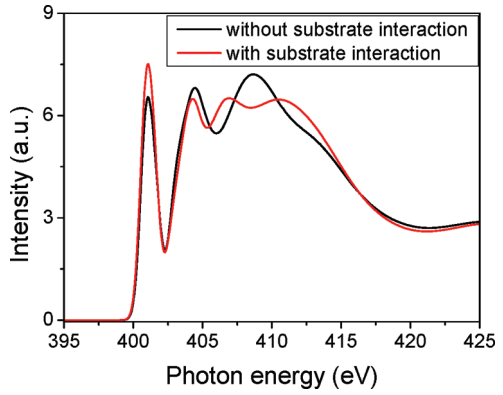

Figure 9. Comparison of calculated NEXAFS spectra showing the effect of inclusion of polymer−substrate interaction.

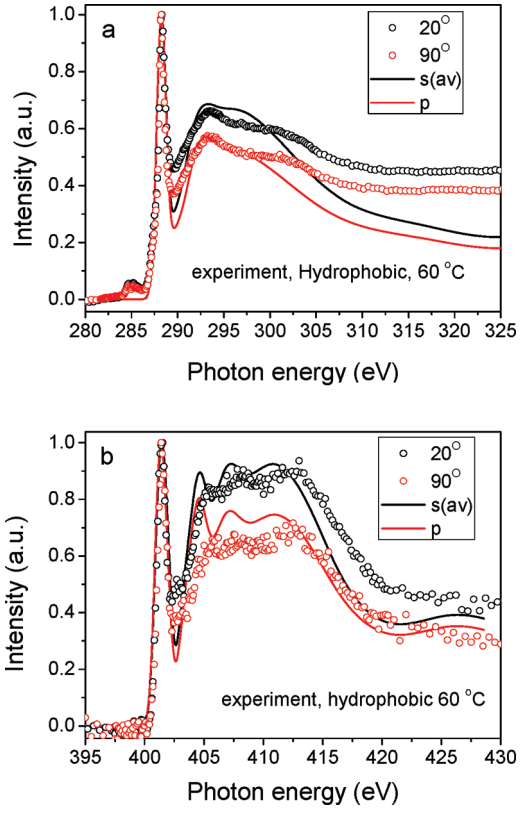

Figure 10. Comparison of experimental and calculated NEXAFS spectra for adsorbed films on hydrophobic substrate (sample 4): (a) C−K edge; (b) N−K edge.

hydrogen atoms observed from the geometry optimization calculation were 3.15, 2.85, and 3.17 Å, which indicate that these are van der Waals type bonds.[38]

It has been observed that the spectra gives the characteristic four-peak structure as observed in the experiment only when the effect of substrate is included in the calculation as shown in Figure 9. Another probable configuration as shown in Figure 8b was also obtained. In this case the CONH plane was parallel to the surface. It is believed that in the actual situation configuration of Figure 8a was more probable compared to that of Figure 8b along with the random ones. Similar to the hydrophilic case, we have calculated the NEXAFS spectra with a combination of 25% oriented with configuration of Figure 8a and 75% of random coils and observed a reasonable agreement with the data. In Figure 10, we have presented the experimental and calculated NEXAFS spectra for films on hydrophobic substrate.

The spin-coated samples were prepared on hydrophilic substrates. From general notion it is expected that the absorption spectra for spin-coated samples should match with those of the films adsorbed on hydrophilic substrate (samples 1 and 3). However, the data shown in Figure 2 appear to have more resemblance with those of adsorbed films on hydrophobic substrate (samples 2 and 4). It may be noted that for adsorption process the polymer chains are free to self-assemble on the substrate according to the mutual interaction between them whereas for spin-coating the polymer molecules are somewhat forced to settle on the substrate. For this reason a better quality film is obtained on hydrophilic substrate by spin-coating as compared to adsorption. Absence of this force in the calculation for spin-coated films therefore leads to incorrect geometry optimization and transition cross-section calculations. As a consequence, NEXAFS spectra could not be calculated to suitably match the experimental data for spin-coated films. Nevertheless, the similarity of the data for the spin-coated films with the calculated spectra for adsorbed films on hydrophobic substrates clearly indicates that strong interaction between the substrate and the polymer molecules are present in this case.

CONCLUSION

In conclusion, we have studied self-assembled PNIPAM films on hydrophilic and hydrophobic substrates. The initial morphology of the polymer chains during self-assembly was controlled by maintaining the solution temperature below and above LCST. Below LCST, the chains are soluble and extended whereas above LCST they are insoluble and globular in nature. The NEXAFS spectra indicate that the polymer chains are oriented similarly on hydrophilic as well as hydrophobic substrate although the chains were having different morphologies in the solution at different temperatures. This indicates that the substrate−polymer interaction plays a dominant role as compared to the intramolecular interaction when the polymer molecules self-assemble on Si substrate. Although NEXAFS data suggest similar morphology on the substrate for both types of surfaces, AFM studies suggest that the morphology of the polymer chains was widely different on hydrophilic substrate compared to the hydrophobic ones. To address these apparent disagreement absorption spectra was calculated using density functional theory. The results show that on hydrophobic substrate polymer−substrate interaction was stronger as compared to that with hydrophilic substrate. However, on both substrates a combination of about 25% oriented and 75% random molecules are found to reproduce the experimental data well. Effect of external force during polymer substrate attachment spin-coated films on hydrophilic substrate were also studied. Our results show that although in case of self-assembly on hydrophilic substrate the polymer−substrate interaction was weak, in case of spin-coated films this interaction plays a dominant role.

AUTHOR INFORMATION

Corresponding Author

*E-mail: manabendra.mukherjee@saha.ac.in.

Present Addresses
[||]Abdus Salam International Centre for Theoretical Physics, Trieste, Italy.

■ ACKNOWLEDGMENT

The work is partially supported by the India—Taiwan program in Science and Technology. We thanks Chia-Hung Hsu of NSRRC for her kind support in accessing the tapping-mode AFM. Author S.M. thankfully acknowledge Dr. Luca Pasquali (Università di Modena e Reggio Emilia) for training him on the STOBE code and the UNESCO and ICTP-TRIL program for financial support for the training. M.M. acknowledges valuable e-mail discussions with L. G. M. Pettersson about use of the code.

■ REFERENCES

(1) Hu, L.; Chu, L. Y.; Yang, M.; Yu, J.; Wang, H. D. *Chem. Eng. Technol.* **2007**, *30*, 523–529.
(2) Jonas, A. M.; Hu, Z. J.; Glinel, K.; Huck, W. T. S. *Nano Lett.* **2008**, *8*, 3819–3824.
(3) Jones, D. M.; Smith, J. R.; Huck, W. T. S.; Alexander, C. *Adv. Mater.* **2002**, *14*, 1130–1134.
(4) Zhou, F.; Shu, W. M.; Welland, M. E.; Huck, W. T. S. *J. Am. Chem. Soc.* **2006**, *128*, 5326–5327.
(5) Filipcsei, G.; Csetneki, I.; Szilagyi, A.; Zrinyi, M. *Oligomers-Polymer Composites-Molecular Imprinting*; Springer-Verlag: Berlin, 2007; Vol. 206, p 137.
(6) Mendes, P. M. *Chem. Soc. Rev.* **2008**, *37*, 2512–2529.
(7) Wang, W.; Troll, K.; Kaune, G.; Metwalli, E.; Ruderer, M.; Skrabania, K.; Laschewsky, A.; Roth, S. V.; Papadakis, C. M.; Müller-Buschbaum, P. *Macromolecules* **2008**, *41*, 3209–3218.
(8) Winnik, F. M. *Macromolecules* **1990**, *23*, 233–242.
(9) Schild, H. G. *Prog. Polym. Sci.* **1992**, *17*, 163–249.
(10) Tam, K. C.; Wu, X. Y.; Pelton, R. H. *J. Polym. Sci., Polym. Chem. Ed.* **1993**, *31*, 963–969.
(11) Tiktopulo, E. I.; Bychkova, V. E.; Ricka, J.; Ptitsyn, O. B. *Macromolecules* **1994**, *27*, 2879–2882.
(12) Wu, C.; Zhou, S. *Macromolecules* **1995**, *28*, 8381–8387.
(13) Wang, X.; Qiu, X.; Wu, C. *Macromolecules* **1998**, *31*, 2972–2976.
(14) Pelton, R. *Adv. Colloid Interface Sci.* **2000**, *85*, 1–33.
(15) Maeda, Y.; Higuchi, T.; Ikeda, I. *Langmuir* **2001**, *17*, 7535–7539.
(16) Stieger, M.; Richtering, W. *Macromolecules* **2003**, *36*, 8811–8818.
(17) Kita, R.; Wiegand, S. *Macromolecules* **2005**, *38*, 4554–4556.
(18) Lutz, J.-F.; Akfemir, Ö.; Hoth, A. *J. Am. Chem. Soc.* **2006**, *128*, 13046–13047.
(19) Bullett, N. A.; Talib, R. A.; Short, R. D.; McArthur, S. L.; Shard, A. G. *Surf. Interface Anal.* **2006**, *38*, 1109–1116.
(20) Bradley, C.; Jalili, N.; Nett, S. K.; Chu, L.; Förch, R.; Gutmann, J. S.; Berger, R. *Macromol. Chem. Phys.* **2009**, *210*, 1339–1345.
(21) Heskins, M.; Guillet, J. E. *J. Macromol. Sci., Chem.* **1968**, *A2*, 1441–1455.
(22) Huber, D. L.; Manginell, R. P.; Samara, M. A.; Kim, B. I.; Bunker, B. C. *Science* **2003**, *301*, 352–354.
(23) Ohya, S.; Sonodaa, H.; Nakayamaa, Y.; Matsudab, T. *Biomaterials* **2005**, *26*, 655–659.
(24) Matsuyama, A.; Tanaka, F. *J. Chem. Phys.* **1991**, *94*, 781–786.
(25) Wu, C.; Zhou, S. *Macromolecules* **1995**, *28*, 5388–5390.
(26) Okada, Y.; Tanaka, F. *Macromolecules* **2005**, *38*, 4465–4471.
(27) Pelton, R. *J. Colloid Interface Sci.* **2010**, *348*, 673–674.
(28) Henke, B. L.; Gullikson, E. M.; Davis, J. C. *Atomic Data and Nuclear Data Tables* **1993**, *54*, 181–342.
(29) WebCrossSections (http://ulisse.elettra.trieste.it/services/elements/WebElements.html) [Online].
(30) STOBE-DEMON version 3.0, 2007 Hermann, K.; Pettersson, L. G. M.; Casida, M. E.; Daul, C.; Goursot, A.; Koester, A.; Proynov, E.; St-Amant, A. Salahub, D. R. Contributing authors: Carravetta, V.; Duarte, H.; Friedrich, C.; Godbout, N.; Guan, J.; Jamorski, C.; Leboeuf, M.; Leetmaa, M.; Nyberg, M.; Patchkovskii, S.; Pedocchi, L.; Sim, F.; Triguero, L.; Vela, A.
(31) Hammer, B.; Hansen, L. B.; Nørskov, J. K. *Phys. Rev. B* **1999**, *59*, 7413–7421.
(32) Perdew, J. P.; Burke, K.; Ernzerhof, M. *Phys. Rev. Lett.* **1996**, *77*, 3865–3868.
(33) Godbout, N.; Salahub, D. R.; Andzelm, J.; Wimmer, E. *Can. J. Chem.* **1992**, *70*, 560–571.
(34) Slater, J. C. In *Advamces in Quantum Chemistry*; Loewdin, P. O., Ed.; Academic: New York, 1972.
(35) Slater, J. C.; Johnson, K. H. *Phys. Rev. B* **1972**, *5*, 844–853.
(36) Kutzelnigg, W.; Fleischer, U.; Schindler, M. *NMR—Basic Principles and Progress*; Springer-Verlag: Heidelberg, Germany, 1990.
(37) Pasquali, L.; Terzi, F.; Seeber, R.; Doyle, B. P.; Nannarone, S. *J. Chem. Phys.* **2008**, *128* (134711), 1–10.
(38) Rowland, R. S.; Taylor, R. *J. Phys. Chem.* **1996**, *100*, 7384–7391.